Experimental Investigation of Forces and Geometry of a Net Cage in Uniform Flow

Pål Furset Lader and Birger Enerhaug

***Abstract*—A scale model of a flexible circular net with different weights attached to the bottom was tested in a flume tank. Global forces and net deformation were measured for different steady current velocities. Three different sizes of bottom weights were used in the tests. The results from these tests are presented and discussed with the emphasis on the dependency between the forces and the geometry. Comparison is also made to empirical based formulas for calculation of drag and lift forces on net structures. Findings show that i) the forces on, and deformation of a flexible net structure are mutually highly dependent on each other; ii) estimates of global forces on a flexible net structure calculated using simple drag formulas derived from stiff net panel experiments give large errors when compared to experimental measurements; iii) numerical models taking into account the dependency between force and deformation should be used to obtain accurate estimates of forces on flexible net structures; and iv) the forces on a flexible net structure are dependent on Reynolds number, and their dependency are similar to that of a regular cylinder.**

***Index Terms*—Flexible structures, hydrodynamics, hydroelasticity, marine structures.**

I. Introduction

major constraint to aquaculture development is the shortage of suitable water space. In Norway, as well as in other countries, this has resulted in an increasing number of fish farms being installed offshore on locations exposed to waves, wind and current. This move toward offshore locations implies that future fish farms most likely will be in the form of large-scale offshore installations, rather than small near-shore farms, and that future farms will be far more exposed to sea loads than most of todays aquacultural installations. The oil and gas industry have over the last decades developed technology for installing structures on highly exposed offshore locations. Aquaculture installations are, in contrast to most oil and gas installations, highly flexible hydroelastic structures. Hydrodynamic forces acting on such a structure affect the shape of the structure, and the altered shape affects the hydrodynamic forces. This complex interaction between load and shape is a typical feature of hydroelastic structures, and makes the understanding of the geometry and forces of net structures very complex and challenging. Before designing, building, and installing offshore aquaculture structures, an understanding of the complex mechanics involved must be achieved trough both experimental investigations, and numerical modeling.

References [1] and [9] developed formulas for drag and lift forces on net structures based on measurements of forces on stiff plane net elements in steady current. These formulas are valid only for a limited range of Reynolds numbers and solidity parameter.

Finite-element models for analysis of the net structure have been developed by several authors. One approach is to model the individual twines in the net using truss elements [3], [11], [8]. Alternatively, the net can be modeled using super elements. [5]–[7] developed a dynamic three–dimensional (3-D) model, based on the load description of plane elements from [1]. The model is initially validated using the results of steady state tests in a flume tank [5], and it is the experimental results from these tests that are presented and discussed in this paper.

II. Experimental Setup

The experiments were conducted at the *North Sea Centre Flume Tank* in Hirtshals, Denmark (Fig. 1). This tank is a vertical-type circular water channel driven by four impellers, with an observation section of 21.3 m × 2.7 m × 8 m (length × height × width). The maximum velocity of the uniform flow is 1 m/s.

The model was composed of a hoop (or ring), a net and a number of weights attached to bottom of the net (Fig. 3). The top of the net was mounted on the hoop so that it took the form of a cylinder with open top and bottom. The hoop was kept in a fixed position during each test. The weights were suspended around the bottom opening of the net, to stretch the net and maintain its shape under the influence of water flow (current). The hoop was made of stainless steel and had an overall diameter of 1.46 m and a rod diameter 0.025 m. The forces and deformation of the netting cylinder were the focus of this study, and the hoop itself was thus designed to have no deformation. The fullscale diameter of the net cylinder is assumed to be 10 m, and the scale is thus 1 : 7.1.

The netting cylinder was made up of two panels which were joined together in the center line of the cage. Each panel was 81 meshes high and 125 meshes wide. With joining meshes included, the total number of meshes in circumferential direction was 252. The netting material was nylon with a mass density of 1130 $\mathrm{kg/m^3}$. The netting was knotless of the *Raschel* type with a nominal bar length of 16 mm and twine thickness of 1.8 mm (Fig. 2). The netting itself was not scaled, and ordinary full-scale netting was used. For the meshes mounted directly to the hoop, the tension applied increased the bar length from 16 to 18 mm. Mounted as square meshes, the solidity (S) of the netting was 0.225. The solidity is defined as the projected area of the twines

Manuscript received July 25, 2003; accepted August 10, 2004. This work was supported by the Norwegian Research Council (NFR) through the research programs "3 Dimensional netpen movement and mooring of fishfarms," and "Modeling and simulation of interaction between fluid and deformable net structures and aquacultural installations." Paper approved by the Guest Editors.

The authors are with SINTEF Fisheries and Aquaculture, 7465 Trondheim, Norway (e-mail: Pal.Lader@sintef.no; Birger.Enerhaug@sin-tef.no).

Digital Object Identifier 10.1109/JOE.2004.841390

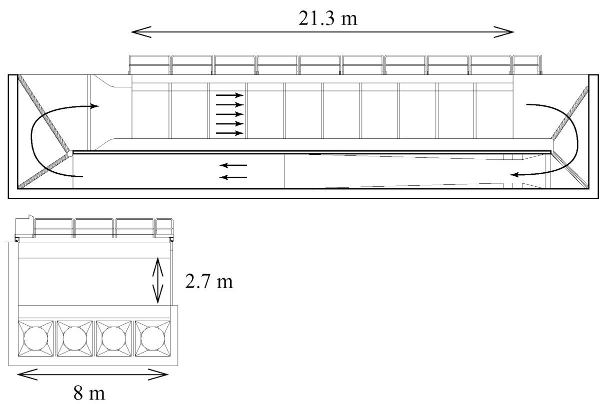

Fig. 1. The *North Sea Centre Flume Tank* in Hirtshals, Denmark. The cross-section area of the measurement section is (8 × 2.7 m).

divided on the total circumscribed area of the nett. The net then formed an open vertical cylinder with diameter 1.435 m and height ca. 1.44 m.

Three sets of 16 weights with nominal mass values of 400, 600, and 800 g were used in the tests. The weights were made of steel and had cylindrical shapes with a diameter of 0.04 m. Three different weight modes (WM) where tested (Table I). The size of the weights corresponds to full scale values of 10, 15, and 20 kg per meter around the circumference of the cylinder.

The general setup is shown in Fig. 3. The hoop with net was positioned in the center line of the tank, approximately 0.9–1.0 m below the surface. The hoop was held in place with four pair of lines to balance the forces from weights and hydrodynamic loads. The equilibrium position of hoop and net was achieved by minutely adjustments of the length and tension in each of the eight lines. Eight load cells using strain gauge technology were used to measure the load in each line. The hydrodynamic forces on the model were found by first calculating the directional unit vectors for all the eight lines. The time series of each force component were then found by multiplying the time series of the eight tensile forces with its appurtenant direction unit vector. The x, y and z force component for each line were summed up into three time series representing the total forces in x, y, and z direction. These forces represent the reaction forces that are needed to balance all the hydrodynamic forces acting on the model. The drag force acting on the hoop itself was measured by running the hoop without the net, and the drag forces on the bottom weights were established by attaching one weight to a thin line and measure the angle of the line as the weight was exposed to current. These forces were then subtracted form the total forces on the model, and the presented measurements of lift and drag are thus the forces acting on the net itself.

The model was subjected to six different current velocity cases ($U_{\mathrm{steady}} \approx 0.04, 0.13, 0.21, 0.26, 0.33, 0.52$ [m/s]). Flow speed was measured with a *Høntzsch Vane wheel A*, which is commonly referred to as a "propeller log." The principle of measurement is that a vane wheel rotates at a speed proportionally to the flow velocity. Because of its little weight, the vane wheel rotational speed adapts quickly to velocity increases. Since the vane wheel is mounted in a nozzle, it measures what can be considered as the horizontal component of the actual flow speed.

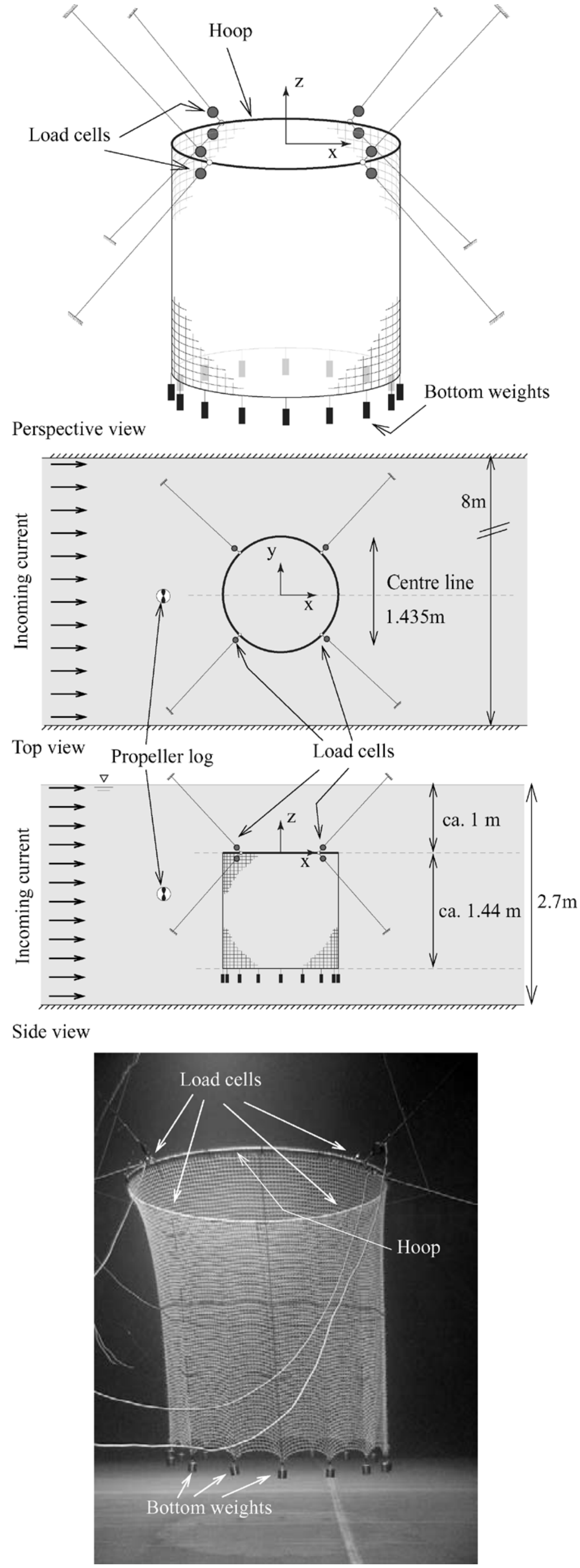

Fig. 2. Netting geometry parameters.

In an aquaculture application, the internal volume of the net structure is influencing the fish health and well being, and it

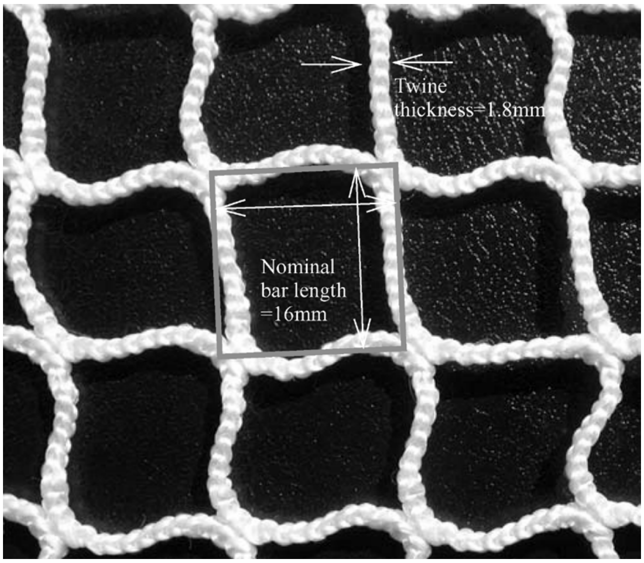

Fig. 3. Model and general setup.

is therefore important to study how the volume is reduced due to current exposure. An estimate of the net geometry was established by measuring the positions of eight markers on the net. The placing and numbering of the markers are shown in Fig. 4. The positions of the markers were measured by a remote controlled video system with an accuracy of ± 5 cm. The position of the markers are used to calculate the volume reduction of the net cylinder. An estimate of the volume reduction is calculated by considering the volume of two prisms with corners 01-03-05-21-23-25 and 21-23-25-41-43-45. The volume of these prisms V_p can be estimated by

$$\begin{aligned} V_p = &\frac{1}{2}(A_{01,03,05} + A_{21,23,25}) \\ &\times \left(-\frac{1}{3}((z_{21} - z_{01}) + (z_{23} - z_{03}) + (z_{25} - z_{05}))\right) \\ &+ \frac{1}{2}(A_{21,23,25} + A_{41,43,45}) \\ &\times \left(-\frac{1}{3}((z_{41} - z_{21}) + (z_{43} - z_{23}) + (z_{45} - z_{25}))\right) \end{aligned} \quad (1)$$

where $A_{n1,n2,n3}$ is the area of the triangle spanned by the points $n1, n2$, and $n3$, and z_n is the z coordinate of point n. The *volume reduction coefficient* (C_{vr}) can be calculated from

$$C_{vr} = \frac{V_p}{V_{p0}} \quad (2)$$

where V_{p0} is the volume of the prisms when the net cylinder is unexposed to current.

The area of the projection of the cylinder onto a plane orthogonal to the incoming current is called the *effective exposed area* (A_e). Due to the deformation of the cylinder, A_e is dependent on the current velocity, and decreases with increasing current. When considering the drag force on the net cylinder the effect of changing A_e should be taken into account. A_e is estimated from the position of the marker points by

TABLE I
WEIGHT MODES

Weight Mode	Weight size	Weight positions
WM1	16 x 400g	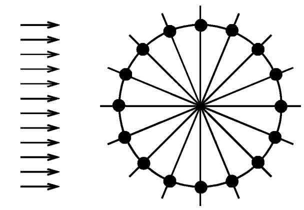
WM2	16 x 600g	
WM3	16 x 800g	

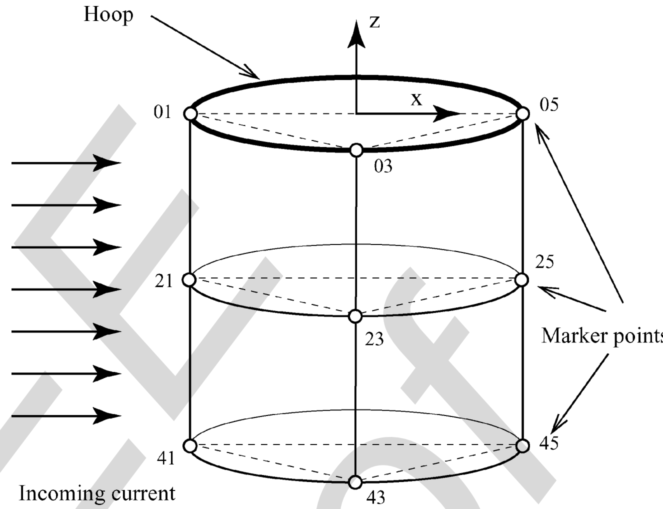

Fig. 4. Placing and numbering of markers on the net cylinder. The coordinate system has its origin at the center point of the hoop, with x axis in the direction of positive current, and z axis upward. The cylinder was assumed to be symmetric about the xz-plane, and only measurements on one side were conducted.

$$\begin{aligned} A_e = 2\Bigg(&- \frac{(y_{03} + y_{23})}{2}(-z_{23} + z_{03}) \\ &- \frac{(y_{23} + y_{43})}{2}(-z_{43} + z_{23})\Bigg) \end{aligned} \quad (3)$$

where y_n and z_n is the y and z coordinates of point n, respectively. The *exposed area reduction coefficient* (C_{ar}) can now be calculated

$$C_{ar} = \frac{A_e}{A_{e0}} \quad (4)$$

where A_{e0} is the effective exposed area when the cylinder is unexposed to current.

III. Results and Discussion

A. Deformation

The deformation of the net cylinder as it is exposed to current is qualitatively described in Fig. 5. From these images the increase in deformation with increasing current velocity can be clearly seen. It can also be observed that increased bottom

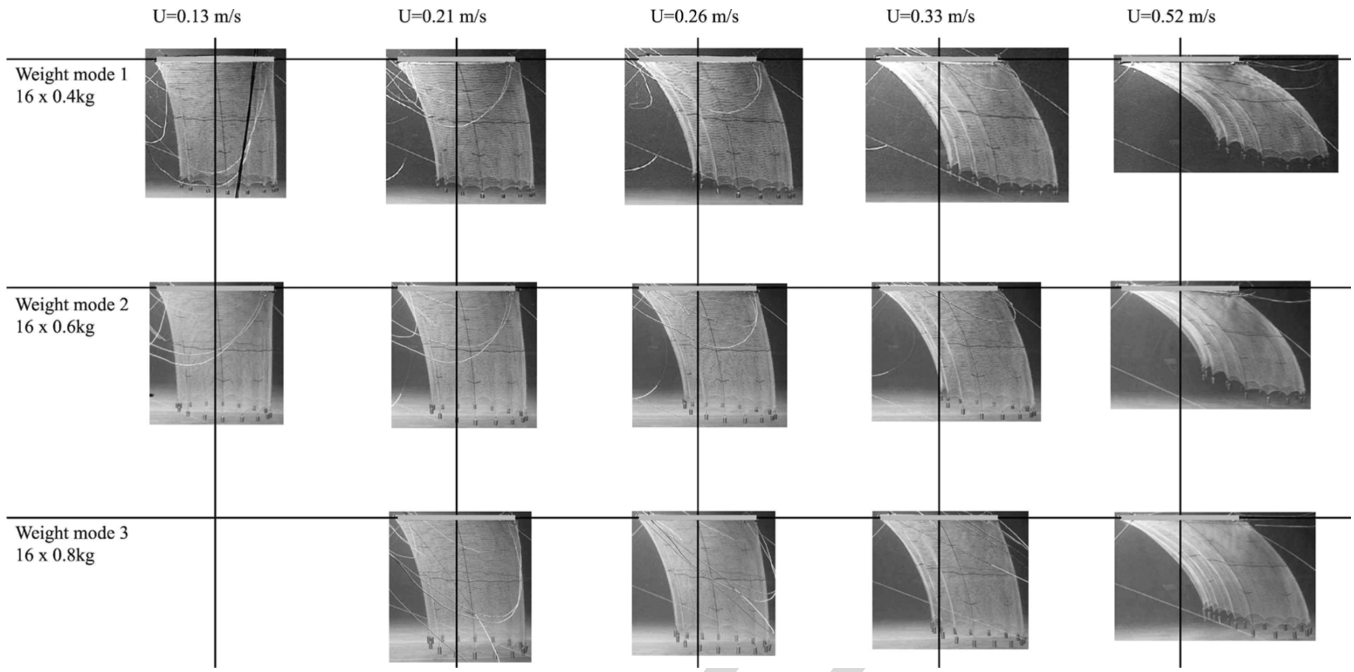

Fig. 5. The deformation of the net cylinder for different weight configurations and current velocities.

weights have a tendency to preserve the geometry. A more quantitative description of the deformation is given in Figs. 6 and 7, where estimates of volume and exposed area reduction are shown. Due to the nature of the measurements technique and calculations of these estimates they have an uncertainty of approximately $pm10\%$.

Both the volume and exposed area reduction show the same qualitative features: For low velocities ($< 0.2\ \mathrm{m/s}$) the deformation is moderate ($< 5\%$), but for higher velocities the deformation becomes substantially larger. The cylinders capability to deform due to increased velocity also increases for higher velocities. However for weight mode 1 it can be seen that the relationship between the velocity and the deformation seems to have an inflection point between 0.26 and 0.33 m/s, and that the cylinder responds less to increased velocity above this point. For increasing velocities the volume and exposed area goes asymptotically toward zero, and since the second derivative for low velocities is negative, an inflection point must also exists for the other two weight cases. Unfortunately, it is outside the velocity area studied here. The position of such an inflection point would be important when deciding on the size of the bottom weights for a fish cage.

B. Force

The drag and lift forces are shown in Figs. 8 and 9. For a stiff net panel it can be assumed that the drag (F_D) and lift (F_L) forces are proportional to U^2, and can be expressed as [9]

$$F_D = \frac{1}{2}\rho C_D A U^2 \tag{5}$$

$$F_L = \frac{1}{2}\rho C_L A U^2 \tag{6}$$

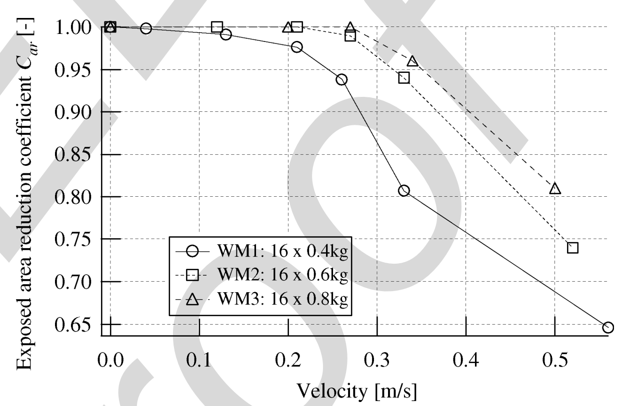

Fig. 6. Exposed area reduction coefficient for the net structure with different weight modes as a function of current velocity.

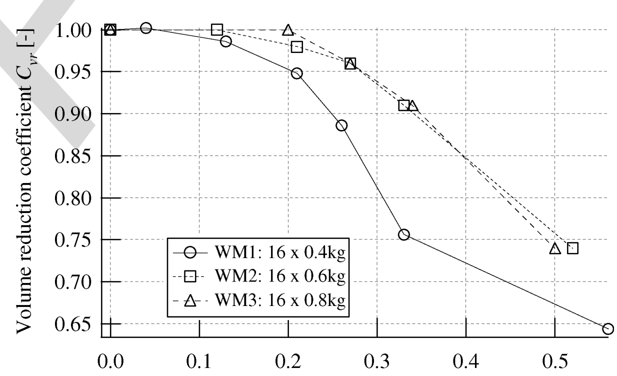

Fig. 7. Volume reduction coefficient for the net structure with different weight modes as a function of current velocity.

where ρ is the density of water, A is the total circumscribed area of the net, U is the current velocity, C_D and C_L are the drag and lift coefficients, respectively, given by

$$C_D = 0.04 + (-0.04 + 0.33S + 6.54S^2 - 4.88S^3)\cos\alpha \quad (7)$$
$$C_L = (-0.05S + 2.3S^2 - 1.76S^3)\sin 2\alpha \quad (8)$$

where S is the solidity of the net, and α is the angle of attack. α is zero when the flowdirection is normal to the panel. The equations are limited to S in the range 0.13 – 0.32.

For flexible structures, as the net cylinder studied here, the global forces are not proportional to U^2 for all velocities. As can be seen from Fig. 8, the drag force seems to have a linear relationship with U for velocities higher than 0.2 m/s. This is due to the deformation of the cylinder, which starts to become significant when U exceeds 0.2 m/s.

When the net structure is flexible the relationship between current velocity and global forces becomes complex since the forces and deformations mutually depend on each other. The force coefficients (7)–(8) depend on net solidity and angle of attack. Both these properties are dependent on the net structure geometry and deformation. Different areas in the net structure have different effective angle of attack, and the effective solidity may be altered due to different tension and compressions in the net.

The difference in drag force for the three weight modes are insignificant for velocities below 0.3 m/s, but the tendency for higher velocities seems to be that the drag increases with increasing bottom weight. This is because increased bottom weights results in decreased deformation of the structure, and thus higher drag force.

The lift force seems to be more dependent on the bottom weight than the drag force. For velocities below 0.4 m/s the lift in the weight mode 3 case is significantly less than the other two cases, while it is significantly higher for velocities of approximately 0.5 m/s. The lift forces on the cylinder are dependent of the local angles (α) of the incoming current to the nett structure and are proportional to $\sin(2\alpha)$ (8). This means that the largest lift force is when $\alpha = \pi/4$. For $U < 0.4$ m/s the angle of the incoming current is larger for weight mode 1 and 2 than for weight mode 3 because they are more deformed, but for a major part of the net structure it is less then $\pi/4$ (as can be observed from Fig. 5). When the velocity increases to 0.5 m/s the major part of the net structure of weight mode 1 and 2 has an angle of incoming current which is higher than $\pi/4$, and consequently experiences a decrease in lift force relative to weight mode 3.

The formulas proposed by [9] are valid for stiff net panels in a steady current. In Fig. 10 a comparison of drag force estimates calculated using (5) and (7) and measurements is shown. The comparison is conducted using weight mode 2 (16×0.6 kg). The drag force is calculated by using (5) where A is the area of the net (equals two times the exposed area A_e since the cylinder has both a front and a rear side), and the angle of attack (α) is assumed to be zero. C_D is then found from $C_D = 0.33S + 6.54S^2 - 4.88S^3$. The drag force is calculated using three different approaches: 1) The exposed area is assumed to be constant equal to A_{e0}, and the front of the cylinder has no shielding effects on the rear side. 2) The effect of the changes in exposed area is taken into account using the measured values. No shielding effects. 3) Shielding effects is taken into account by assuming the current velocity on the rear side of the cylinder to be 0.8 times the incoming current velocity (based

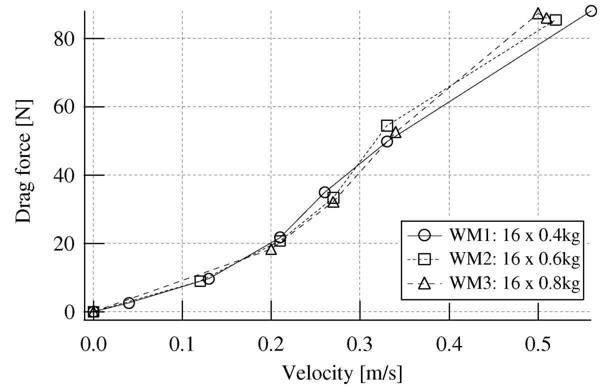

Fig. 8. Drag force on the net structure with different weight modes as a function of current velocity.

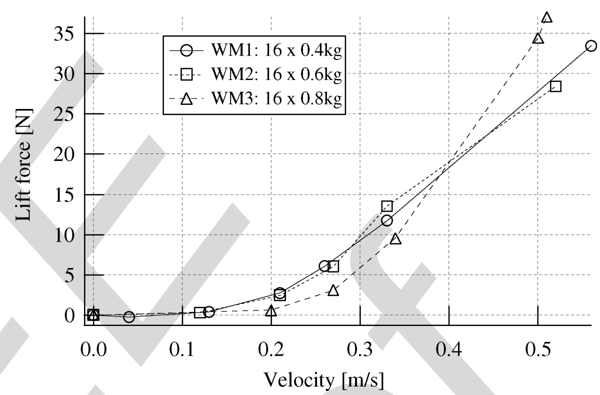

Fig. 9. Lift force on the net structure with different weight modes as a function of current velocity.

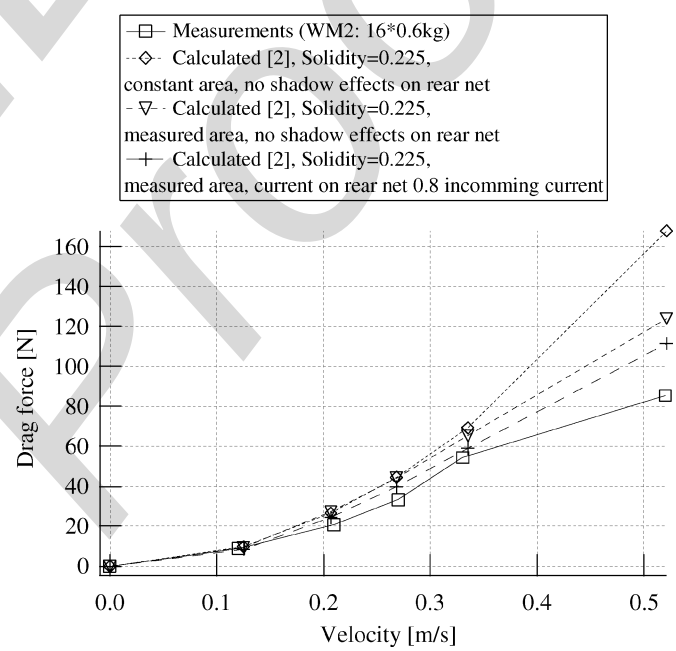

Fig. 10. Comparison of measured drag force with calculated drag force using the formulas found by [9].

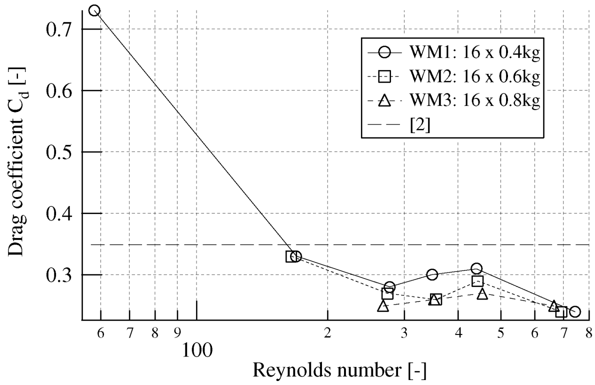

Fig. 11. Effective drag coefficient calculated from the measurements of drag force and effective exposed area for different Reynolds number. The twine diameter is used as the characteristic diameter in the Reynolds number. The drag coefficient calculated using (7) [9] is shown for comparison (dashed line). The drag coefficient found by [9] was based on measurements with a Reynolds number in the area 1400–1800.

on measurements of the current inside the cylinder). When compared to the measured drag force the calculations all deviate considerably from the measurements, and overpredict the drag force. This shows the difficulty of using crude calculations based on simple formulas when calculating the forces on flexible net structures. Possibly the only way to obtain good estimates of forces is to use numerical models which take into account the dependency between the deformation and the forces.

Another problem with using (7) and (8) is that they are independent of Reynolds number (R_n). The net structures basic components are the twines, and the net can be assumed to be made up of an array of cylinders, even though the twine connections have considerable contributions on the forces for solidity above 0.3 [2]. The drag force on cylinders are dependent on R_n, and the drag force on net structures are thus also dependent on R_n [2]. Based on the drag measurements and the measurements of exposed area, an estimate of effective drag coefficient can be made using (5). The net area A in the equation is the measured exposed area. The drag coefficients as a function of Reynolds number are shown in Fig. 11. The drag coefficient calculated using (7) is also shown in the figure (dashed line). As expected, the drag coefficient shows a dependency on R_n which is significant. For low R_n the drag coefficient shows an increasing tendency as also found by [4], not unlike drag coefficients on regular circular cylinders [10]. For R_n in the range 200–800, the drag coefficient from (7) overpredicts the drag force, as observed earlier in Fig. 10.

IV. Conclusion

The forces on, and deformation of a flexible net structure are mutually highly dependent on each other.

Estimates of global forces on a flexible net structure calculated using simple drag formulas derived from stiff net panel experiments give large errors, when compared to experimental measurements.

Numerical models taking into account the dependency between force and deformation should be used to obtain accurate estimates of forces on flexible net structures.

The forces on a flexible net structure are dependent on Reynolds number, and their dependency are similar to that of a regular cylinder.

References

[1] J. V. Aarsnes, G. Løland, and H. Rudi, "Current forces on cage, nett deflection," in *Engineering for Offshore Fish Farming*. Glasgow, U.K.: Thomas Telford, 1990, pp. 137–152.

[2] A. Fredheim and O. M. Faltinsen, "Hydroelastic analysis of a fishing net in steady inflow conditions," in *3rd Int. Conf. Hydroelasticity in Marine Technol.*, Oxford, U.K., 2003.

[3] D. W. Fredriksson, M. R. Swift, J. D. Irish, I. Tsukrov, and B. Celikkol, "Fish cage and mooring system dynamics using physical and numerical models with field measurements," *Aquacultural Eng.*, vol. 27, no. 2, pp. 117–146, 2003.

[4] A. L. Fridman and P. J. G. Carrothers, *Calculations for Fishing Gear Designs*. Farnham: Published by arrangement with the Food and Agriculture Organization of the United Nations by Fishing News Books, 1986.

[5] P. Lader, B. Enerhaug, A. Fredheim, and J. R. Krokstad, "Modeling of 3D net structures exposed to waves and current," in *3rd Int. Conf. Hydroelasticity in Marine Technol.*, Oxford, U.K., 2003.

[6] P. Lader and A. Fredheim, "Modeling of net structures exposed to 3D waves and current," in *Open Ocean Aquaculture IV*, St. Andrews, Canada, 2001.

[7] P. Lader, A. Fredheim, and E. Lien, "Dynamic behavior of 3D nets exposed to waves and current," in *20th Int. Conf. Offshore Mechan. Arctic Eng.*, Rio de Janeiro, Brazil, 2001.

[8] F. Le Bris and D. Marichal, "Numerical and experimental study of submerged supply nets: Applications to fish farms," *J. Marine Science Technol.*, vol. 3, pp. 161–170, 1998.

[9] G. Løland, "Current forces on and flow through fish farms," Dr.ing., Division of Marine Hydrodynamics Norwegian Institute of Technology, Trondheim, Norway, 1991.

[10] H. Schlichting, *Boundary-Layer Theory*. New York: McGraw-Hill, 1979.

[11] I. Tsukrov, O. Eroshkin, D. Fredriksson, M. R. Swift, and B. Celikkol, "Finite element modeling of net panels using a consistent net element," *Ocean Eng.*, vol. 30, no. 2, pp. 251–270, 2003.

Pål F. Lader was born in Kristiansund, Norway, in 1969. He received the M.Sc. degree in marine technology in 1993 and the Ph.D. degree in marine hydrodynamics in 2002 from The Norwegian University of Science and Technology. His Ph.D. work was an experimental study of breaking waves using the particle image velocimetry (PIV) method.

Since 1999 he has been a Research Scientist with the SINTEF Fisheries and Aquaculture Research Institute. His research is now mainly focused on the hydroelastic behavior of flexible netting structures in waves and current.

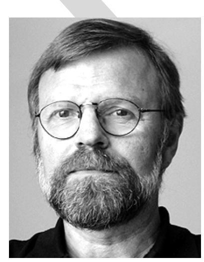

Birger Enerhaug was born in Haram, Norway, in 1948. He received the B.S. degree in naval architecture from the Oslo College of Naval Architecture, Norway, in 1971, and the M.S. degree, also in naval architecture (marine hydrodynamics), from The Norwegian Institute of Technology in 1975.

He worked as a research scientist with The Institute of Fisheries Research (FTFI) from 1976 to 1990. From 1990 to 1999, he was a Senior Research Engineer with The Norwegian Marine Technology Research Institute (MARINTEK). Since 1999, he has been a Senior Scientist with the SINTEF Fisheries and Aquaculture Research Institute. His research fields are sea-keeping qualities of fishing vessels and hydrodynamics of fishing gears.